Co-generation of Carbon-Free Hydrogen and Electricity from Coal in a Steam-Carbon Fuel Cell with Carbon Capture

GCEP 2013 Progress Report

Submitted by:

Professor Reginald E. Mitchell
Principal Investigator
Department of Mechanical Engineering
Stanford University

and

Consulting Professor Turgut M. Gür
Co-Investigator
Department of Materials Science and Engineering
Stanford University

April 29, 2013

Investigators

Reginald E. Mitchell, Professor, Mechanical Engineering, Principal Investigator
Turgut M. Gür, Consulting Professor, Materials Science and Engineering, Co-PI
David U. Johnson, Kevin Steinberger, Graduate Researchers
Brentan Alexander (Ph.D: Aug. 2012) and Gregory Armstrong (MS: June 2012)

Stanford University, Stanford, CA 94305

Abstract

This new project, initiated about a month ago, collectively aims to address three aspects of energy production and storage using coal, namely, advanced coal conversion in a specialized fuel cell, electrochemical hydrogen production from coal for energy storage, and CO_2 mitigation and capture without separation, all achieved in a single process chamber and without the need for external power from the grid. If successful and widely adopted, this technology could result in a significant reduction in global CO_2 emissions over the long term with continued use of coal, our cheapest and most abundant fuel.

The steam-carbon fuel cell [1] introduced in this project is a novel concept that not only achieves steam gasification of coal while keeping hydrogen and carbon dioxide product streams unmixed and physically separated by an imprevious ceramic membrane, but more importantly, drives the otherwise thermodynamically uphill reaction for steam dissociation energetically downhill. The oxygen needed to oxidize the carbon-containing fuel at the anode is derived from the splitting of steam at the cathode and is transported as oxide ions through the crystal lattice of the ceramic membrane, while the elecrons travel through the external circuit (or, grid) performing useful electrical work. In this process scheme, no nitrogen enters the reaction stream so the anode product gases contain primarily CO_2 and unreacted CO, while the cathode gas stream contains primarily H_2 and unreacted steam. In other words, the steam-carbon fuel cell concept enables simultaneous and spontaneous production of carbon-free hydrogen and electricity from coal (or biomass) and produces a highly concentrated CO_2 product stream that can easily be captured.

An added innovation in this project involves development of solid sorbent materials for *in situ* capture and removal of coal contaminants, mainly sulfur, inside the same reaction chamber that houses the steam-carbon fuel cell. Such an advancement is critically important towards practical realization of coal conversion in carbon fuel cells where coal contaminants pose difficult challenges making it almost impossible to utilize coal-drived syngas without extensive pretreatment and syngas cleaning.

Another innovation of the project involves physical and thermal coupling of an air-coal fuel cell with the self-driven steam-carbon fuel cell to both augment and provide increased flexibility for load leveling and centralized or distributed power generation, as well as increased hydrogen production for large scale energy storage applications. The coupled fuel cell approach with *in situ* sulfur removal offers a significant breakthrough in the utilization of coal and has the potential to change the landscape for both clean coal power generation as well as the production of carbon-free hydrogen, important for transportation applications.

A preliminary modeling study [2] based on unoptimized experimental data indicated that the coupled fuel cell scheme can efficiently and spontaneoulsy produce both hydrogen and electrical power without any external heat input, and promises the potential for overall system efficiencies up to 78% while simulatneously producing hydrogen at a rate of 1.22 kg/m^2 per day and electrical power at 45 mW/cm^2.

Introduction

This project is built upon the steam-carbon fuel cell concept [1-4] and involves conversion of coal or biomass at the anode while hydrogen from the reduction of steam is produced at the cathode. The two reaction systems are separated by an oxide ion conducting ceramic membrane. In other words, this scheme in essence allows the water gas shift reaction and the steam gasification reaction of coal to be achieved in such a way that the anode and cathode reaction streams do not mix with each other, minimizing entropic losses. Furthermore, the favorable thermodynamics of this system allows spontaneous and simultaneous production of hydrogen and electrical energy. The downhill driving force facilitates a large difference in the chemical potential for oxygen across the ceramic membrane, whereby oxygen is abstracted from steam at the cathode, transported via vacancy mechanism across the crystal lattice of the membrane towards the anode where it reacts with the carbonaceous fuel [5]. The electrons released at the anode travel through the external circuit to perform useful electrical work. This novel scheme offers efficient and cost-effective production of carbon-free hydrogen and electrical power.

The goal of the project is to gain mechanistic and operational understanding of a novel fuel cell concept that represents a game-changing opportunity to achieve highly efficient conversion of coal and biomass in fuel cells on practical scales with simultaneous and spontaneous production of electricity and carbon-free hydrogen. The research effort involves experimental, materials, and modeling components. Laboratory experiments are designed to provide the information needed to characterize mass transport and electrochemistry at the cathode and anode of the steam-carbon fuel cell as well the heterogeneous gasification reactions that occur in the fluidized bed of coal particles, producing the synthesis gas that is oxidized at the anode. Catalytic materials will be investigated for improving electrode kinetics at the anode and cathode, while materials strategies will be developed to address the deleterious effects of coal contaminants, primarily sulfur. Models developed to describe the observed phenomena will be implemented to gain fundamental understanding in the areas of coal gasification, carbon monoxide electrochemistry and steam electrolysis. System optimization will also be an aspect of the continuing research. Understanding challenges in system scaling, thermal management, power management, and membrane electrode assembly designs, especially for multi-cell configurations are key concerns. If successful and widely adopted, the technology would greatly reduce greenhouse gas emissions during the production of high-purity hydrogen and electricity from coal and biomass.

The impacts of this research project are in the areas of efficient energy conversion (coal) and storage (hydrogen) with reduced carbon footprint, as well as in the education of students in advanced approaches to energy and environment for a sustainable future.

Background

As an environmentally clean energy carrier, hydrogen has the potential to become a significant player especially in the transportation sector. Development efforts by major automobile manufacturers towards fuel cell driven vehicles, if commercially successful, necessitates parallel efforts in developing cost effective technologies for distributed production and availability of carbon-free hydrogen.

Molecular hydrogen, found only in trace quantities in nature, must be synthesized from hydrogen-containing compounds such as water or hydrocarbons. The production of hydrogen by steam reforming is a mature technology that accounts for more than 75% of the current production capacity, but is cost effective only when it is produced centrally and at large scale. Storage and transportation of hydrogen, however, is costly and inefficient. That is why distributed generation will be important and the development of novel H_2 synthesis processes with low energy consumption and minimum greenhouse gas emissions is critically needed. If an effective hydrogen-based clean transportation economy is to be developed, then distributed production of hydrogen from coal is a viable low-cost option.

Currently, the conventional room temperature electrolysis of water is the only commercial technology available for distributed generation of hydrogen. But thermodynamically this is steeply an uphill process and hence, is energy intensive. An external bias of about 1.8 - 2 V that opposes and is significantly greater than the open circuit voltage of 1.23 V must be applied to the cell in order to break the O-H bonds in water, permitting the formation of the H-H bond. In other words, 60% to 70% of the electricity used in conventional water electrolysis schemes is consumed merely to overcome this potential barrier and overdrive the cell uphill. This reduces the efficiency and renders electrolysis an inefficient, costly process for distributed hydrogen production. Considering that nearly 50% of the global grid power is generated primarily by coal fired plants operating at conversion efficiencies in the low 30% range, the overall efficiency of conventional water (or, steam) electrolysis is further reduced significantly by this efficiency multiplier.

The fuel cell scheme adopted in this project for hydrogen production is different from and much superior to conventional electrolysis, and is expected to be nearly two times more efficient. In this innovative scheme, H_2O dissociation and fuel (*i.e.,* carbon) oxidation processes are coupled and the resulting net reaction is thermodynamically downhill. In other words, the dissociation reaction for steam occurs spontaneously. So no electricity from the external power grid is required or needed, which results in big savings in electrical energy consumption. Moreover, the cell operates at high temperatures where the open circuit potential for steam dissociation is lower (0.9 V for water at 1200 K versus 1.23 V for water at room temperature), and electrode kinetics and fluxes are much faster. Indeed, Doenitz *et al.* [6] have demonstrated steam electrolysis using a solid oxide electrolyzer at applied biases in excess of 0.9 V in the range 900 – 1000˚C.

This fuel cell scheme is also distinctly different from steam reforming of hydrocarbons and various coal and biomass gasification processes for hydrogen production, where the hydrogen produced is provided from both the steam and the hydrocarbon or the coal or biomass. By contrast, in this project, the hydrogen is

supplied solely from water, not the coal. In addition, unlike steam reforming and gasification processes, which require energy intensive separation steps to recover H_2 and remove CO_x gases down to trace quantities, the two streams in this project do not mix and are physically separated at all times by the impervious ceramic membrane. The resulting cathode product gas is pure H_2 with unreacted steam, but no contamination from CO_x gases. Water can easily be condensed to produce a high-purity hydrogen product stream for use as an energy carrier for large scale storage or an effective fuel for polymer exchange membrane fuel cells (PEMFC) for transportation application. Carbon-free purity is a critical consideration for near-room temperature hydrogen fuel cell applications, where even trace levels of CO in the H_2 fuel feed may be detrimental to the operation and long term performance of the fuel cell due to catalyst deactivation.

Another advantage offered by this project is that carbon dioxide is used to gasify the coal bed instead of steam that is otherwise used typically in all coal gasification applications. Use of CO_2 minimizes the coking problems that have hindered previous attempts to immerse solid oxide fuel cells in steam gasified carbon beds.

This project provides a significant innovation towards total independence from the electricity grid by thermally and physically coupling a steam-carbon fuel cell directly with an air-carbon fuel cell (as shown in Fig. 1), such that the two cells share the same coal/biomass bed as the anode compartment while the corresponding cathode compartments contain steam and air, respectively. The coupled fuel cell arrangement allows simultaneous and spontaneous production of electrical power and carbon-free hydrogen, such that the production amounts of each can be adjusted at will based on the relative demands for power generation or chemical storage. In addition to such flexibility, this scheme offers several important advantages, namely, 1) efficient generation of power during peak demand times for load leveling, 2) large-scale chemical storage of electrical energy at off-peak times in hydrogen which is an effective and clean energy carrier, 3) reduced emissions of CO_2 into the environment, 4) production of highly concentrated CO_2 (> 90%) in the flue gas that eliminates the need for separation from nitrogen, and 5) distributed generation of power and hydrogen from local resources such as biomass.

Our efforts aim to characterize and understand the underpinning science and technology of this approach using laboratory-scale experiments and modeling. Of specific concern are the identification of anode materials that (i) are stable in reducing environments containing solid carbon, (ii) have high catalytic activity towards the oxidation of carbon and CO, (iii) can tolerate trace levels of sulfur, (iv) have suitable mechanical and microstructural stability, and (v) are not expensive. Materials that form stable, durable, and catalytically active cathodes that enhance charge transfer rates for steam decomposition and oxygen reduction need to be identified.

Another objective of this research project is to develop a scheme to reduce the sulfur levels in the carbon bed to parts-per-million levels, levels that fuel cell anodes can tolerate for long periods without significant degredation. Coal contaminants, in particular sulfur-containing compounds, are known to deactivate and posion fuel cell anodes. Accordingly, efforts aim to investigate, identify and develop regenerative sulfur sorbents for *in situ* sulfur removal as well as to develop suitable anode

materials that exhibit sufficient tolerance for trace levels of sulfur (<5 ppmv) without significant degradation in fuel cell performance.

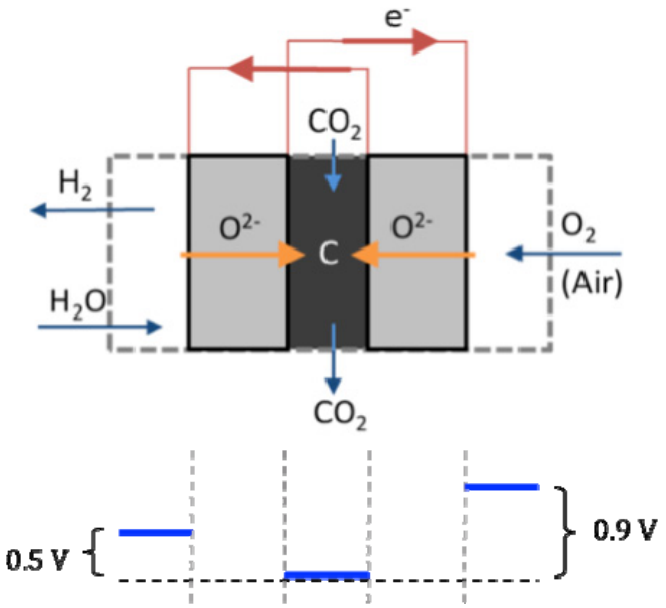

Figure 1: Schematic of a coupled steam-carbon and air-carbon fuel cell, and the corresponding oxygen chemical potential profile across the coupled cell.

The coupled fuel cell scheme is inherently suitable for large-scale applications. A 25 kW scale solid oxide fuel cell power plant is under development by the industrial teams in the U.S. Department of Energy's Solid State Energy Conversion Alliance (SECA) program and 2 - 5 kW level power units have already been tested [7]. Estimates indicate higher efficiency and significant benefits in capital cost and cost of electricity when integrated gasification fuel cell technology is compared to other coal conversion technologies. Large-scale projects include DOE's FutureGen 2.0 initiative and the GreenGen project in China. Also, Gür and co-workers have recently demonstrated successful operation of a 50-cell stack running on CO fuel and providing nearly 1.2 kW of power or 224 mW/cm^2 power density at 800 ^{o}C [8]. Furthermore, Gür *et al*. [9] have achieved practical power densities up to 450 mW/cm^2 at 0.64 V and 850 ^{o}C using untreated Alaska coal char in a fluidized bed carbon fuel cell, similarly operating under the same basic principle as studied here. Recently, we have demonstrated the fluidized-bed carbon fuel cell (FB-CFC) in which a tubular solid oxide fuel cell (SOFC) is immersed in a bed of carbon particles [5,10]. In another configuration involving flat button-cell geometry, current densities as high as 275 mA/cm^2 at 0.516 V (maximum power: 142 mW/cm^2) were realized at 900 ˚C [5].

Results

At the time of this report, the project has been officially in effect for only a month (*i.e*., since March 2013) and hence, we cannot yet offer substantial results. However,

in anticipation of a possible project award, we have conducted some preliminary studies.

Preliminary Coupled Cell Experiments

To emulate the basic concept of the coupled cell schematically depicted in Figure 1, two separate fuel cells, one air-carbon and another steam-carbon, were constructed and tested at 900°C. The configurations of the two cells can be represented as,

Air-carbon cell: $O_{2(g)}/LSM/YSZ/Ni/C_{(s)}, CO, CO_2$ (1)

Steam-carbon cell: $C_{(s)}, CO, CO_2/Ni/YSZ/Ni/H_2O_{(g)}, H_2$ (2)

The cathode reaction in the air-carbon fuel cell is the electrochemical reduction of oxygen by

$$O_2 + 4e^- = 2O^{-2} \quad (3)$$

and the cathode reaction in the steam-carbon fuel cell is the electrochemical reduction of steam by

$$H_2O + 2e^- = H_2 + O^{-2} . \quad (4)$$

The primary anode reaction for both the air-carbon and steam-carbon fuel cells is the electrochemical oxidation of carbon monoxide by

$$2CO + 2O^{-2} = 2CO_2 + 4e^- \quad (5)$$

and the carbon monoxide consumed at the anode is generated in the fuel bed within the anode compartment through the Boudouard reaction,

$$C_{(s)} + CO_2 = 2CO \quad (6)$$

Oxide ions formed during the reduction of oxygen or steam at the corresponding cathode migrate downhill through the YSZ electrolyte via lattice vacancies and electrochemically oxidize the CO at the anodes. As the oxidation product CO_2 diffuses out into the solid fuel bed, a portion will undergo further gasification through the Boudouard reaction generating CO, some of which is then oxidized at the anode. This so-called "CO shuttle" mechanism was recently proposed by Gür [11] to account for the operating principle of many previous studies using similar cell arrangements [12-15]. The net reaction for the air-carbon and steam-carbon cells, containing both the anode and cathode half cell reactions as well as the carbon bed gasification reaction for each cell, can summarily be respectively written as

$$O_2 + C_{(s)} = CO_2 \quad (7)$$

$$2H_2O + C_{(s)} = CO_2 + H_2 \quad (8)$$

Reaction (7) is, in effect, the carbon combustion reaction, and reaction (8) is, in effect, the carbon steam gasification reaction to form syngas coupled with the water-gas shift reaction, however the completion of the reactions in the coupled fuel cell arrangement leads to four electrons traversing an external circuit for each carbon atom consumed in the bed. The presence of a solid carbonaceous fuel in the anode chamber results in lowering of the oxygen activity at the anode surface, as a portion of the carbon dioxide eluting from the anode surface is reacted to form carbon monoxide via the reverse Boudouard reaction.

The thermodynamic driving force presented in Fig. 2 for these two cells can be directly calculated from fundamental thermodynamic principles using the Nernst Equation in combination with the Boudouard equilibrium concentrations of carbon monoxide and carbon dioxide in the anode chamber.

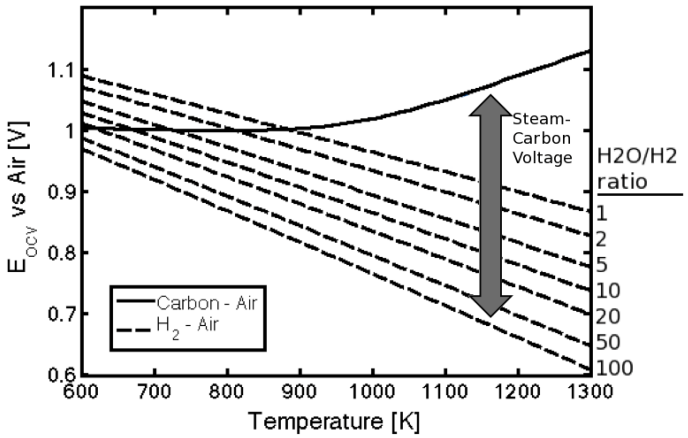

Figure 2: Thermodynamic open circuit voltages for an air-carbon and air-hydrogen cell. The differences between the solid and dashed lines represent the expected open circuit voltage for a steam-carbon cell.

To simulate a steam-carbon-air coupled cell, the experimental air-carbon and steam-carbon cells were electrically connected in series with a galvanostat and in parallel to a potentiostat. By varying the voltage and measuring the current response, the coupled cell was interrogated with the potentiostat/galvanostat and the resultant current-voltage behavior of the combined cells was measured. The results of these measurements are shown in Fig. 3 for a cell temperature of 900° C. Positive voltage is measured according to the steam-carbon cell, and therefore negative voltages correspond to an overdriven steam-carbon cell.

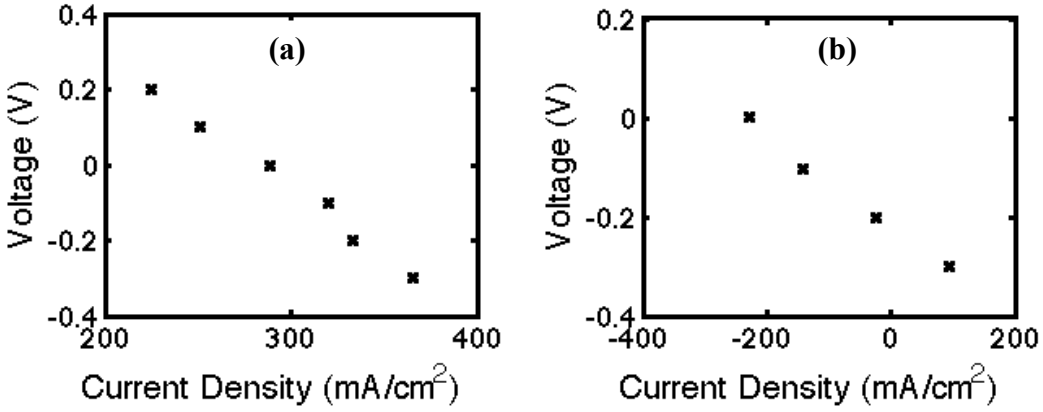

Figure 3. The DC current-voltage response of the coupled steam-carbon-air test cell at 900° C with (a) the galvanostat connected in series and with (b) the potentiostat connected in parallel. Positive voltage is according to the steam-carbon half of the cell.

The results indicate that the coupled cell is capable of spontaneously generating both hydrogen and electricity. When the cells are connected directly together and no power is removed via a series or parallel load, the air-carbon half of the cell is capable of holding the steam-carbon half of the cell at -0.2 V, producing an overall current density of 330 mA/cm^2 in both cells. This current density is equivalent to the short circuit current density of the steam-carbon cell at 1000° C, and is nearly twice the short circuit current density for the steam-carbon cell at the operating condition of 900° C.

The individually measured I-V data of the two cells are combined in Fig. 4, which agree well with the behavior shown in Fig. 3. An example line, labeled 'series reading', is shown at a current density setting of 120 mA/cm^2. The expected readout is the vertical difference at this point, or roughly 0.4 V. A similar prediction for a current density of 400 mA/cm^2 places the expected reading at -0.4 V, which matches well with the measured result in Figure 3a.

Similarly, when the potentiostat is connected in parallel with the coupled cells, as in Fig. 3b, the expected reading at any chosen voltage is the horizontal difference between the two cell I-V curves. This prediction is shown in Fig. 4 as a horizontal line labeled 'parallel reading.' For a potentiostatic setting of -0.1 V, the expected output based on the horizontal difference in Fig. 4 is approximately -160 mA/cm^2, which matches well with the actual measured value in Fig. 3b of -172 mA/cm^2.

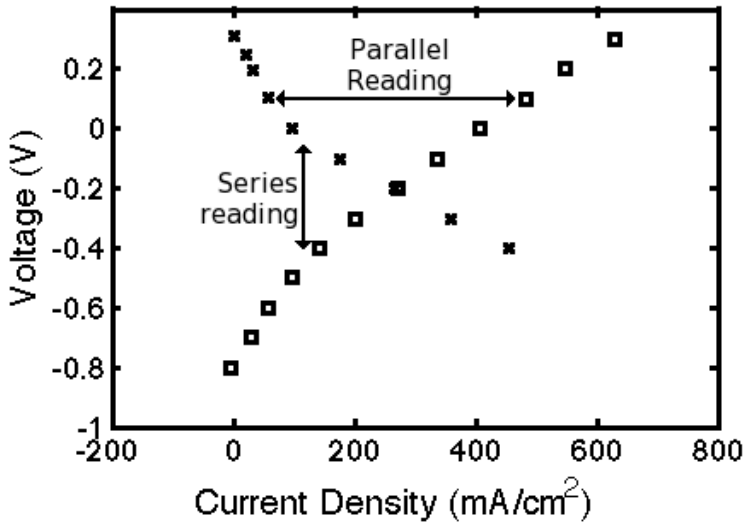

Figure 4: Independent I-V response of the air-carbon (squares) and steam-carbon (x) cells. The intersection is the expected operation point of a coupled cell with no external power outputs or inputs. The 'parallel reading' line indicates that the current density that is expected to be measured by a potentiostat attached in parallel is the horizontal difference between the two I-V curves (shown at 0.1 V setting on the potentiostat), and the 'series reading' line indicates that the expected reading on a galvanostat connected in series to these cells would be the vertical difference between the two I-V curves (shown at 120 mA/cm^2 setting on the galvanostat).

Preliminary Coupled Cell Modeling Study

To explore the operating space of the couple fuel cell and determine the interplay between overall cell efficiency, hydrogen production rate and electricity production rate, a preliminary model was developed for the combined cell to predict operating parameters under a given set of conditions. The model is based on previous work from our laboratory on the Boudouard reaction mechanism and kinetic parameters for an activated carbon fuel, which is used in this study [16].

To model the global gasification reaction (Reaction (5)) occurring in the fuel bed, the Boudouard mechanism put forth by Ma is used [17]. This mechanism is listed in Table I, and is made up of five elementary reactions, two of which can also occur in reverse, that previous work in our lab has shown to effectively model Boudouard gasification kinetics. In the table, C_f represents a free surface carbon site, C(k) is a carbon site with species k adsorbed on the surface, and C_b represents a carbon atom in the bulk of the material. Reaction 1f and Reaction 2, which govern the adsorption of oxygen onto the carbon surface and the reaction of adsorbed oxygen to form CO, respectively, are the rate-limiting and most important reactions in this mechanism. The Arrhenius form was assumed for each reaction, yielding a set of kinetic parameters consisting of seven pre-exponential terms, A, and seven activation energies, E, that completely describe the mechanism for any given carbonaceous fuel.

Table I: Boudouard Reaction Mechanism [17]

Reaction
1f: $C_f + CO_2 \rightarrow C(O) + CO$
1r: $C(O) + CO \rightarrow C_f + CO_2$
2: $C_b + C(O) \rightarrow CO + C_f$
3: $C_b + C(O) + CO_2 \rightarrow 2\ CO + C(O)$
4f: $C_f + CO \rightarrow C(CO)$
4r: $C(CO) \rightarrow C_f + CO$
5: $CO + C(CO) \rightarrow CO_2 + 2\ C_f$

The activated carbon fuel used in the experimental setup is used in this model, and its kinetic parameters were found through a series of experiments in a thermogravimetric analyzer facility (TGA). The kinetic parameters of reactions 2 and 4r were determined directly through temperature programmed desorption (TPD) measurements for loading atmospheres of CO and CO_2. The theoretical development of Brunauer, Emmett and Teller (BET), which applies Langmuir adsorption theory to multiple layers of gas phase adsorbing species onto an active surface, was used to determine the specific surface area of the char [18,19]. The CO_2 partial pressure in the environment surrounding a char sample was adjusted in step intervals over time, and the mass changes of the char particles were measured. Multiple BET measurements were performed at different extents of char conversion, yielding both an initial specific surface area, $S_{g,C,0}$, and a structural parameter, ψ, that can be used to predict the specific surface area, $S_{g,C}$, as a function of char conversion according to the function derived from the results of Bhatia and Perlmutter [20]. The remaining kinetic parameters were found by fitting the reaction mechanism to the TGA datasets.

These kinetic parameters were utilized in an axisymmetric finite element model of the carbon char bed. The bed is divided into a sufficient number of interconnected differential volume elements in which the carbon particles are uniformly dispersed. The carbon particles are assumed fixed and confined to the volume elements, while gaseous species flow by convective and diffusive processes throughout the bed. The gas phase mass conservation in the bed, coupled with Darcy's Law, gives

$$\nabla \cdot (\rho \vec{u}) = S_{g,C} \frac{M_C}{V_{free}} \left(\hat{M}_{CO} \hat{R}_{CO} + \hat{M}_{CO_2} \hat{R}_{CO_2} \right) \tag{9}$$

where ρ is the gas density, $S_{g,c}$ is the specific surface area of the activated carbon, M_C is the total mass of carbon in the bed, V_{free} is the total gas phase volume available in the bed, (defined as the total reactor volume minus the volume occupied by carbon particles), and $\hat{M}_{CO}$ and $\hat{M}_{CO_2}$ are the molecular weights and $\hat{R}_{CO}$ and $\hat{R}_{CO_2}$ are the reaction rates of CO and CO_2, respectively, calculated using the local CO and CO_2 concentrations and the reaction mechanism shown in Table 1. The convective velocity is given by

$$\vec{u} = -\frac{\kappa}{\mu} \nabla P \tag{10}$$

where the bed permeability κ is estimated using the Blake-Kozeny equation [21]

Gas transport through the bed is described for both CO and CO_2 by using the species conservation equation

$$\nabla \cdot \left(-D_{eff} \nabla C_i + C_i \vec{u} \right) = S_{g,C} \frac{M_C}{V_{free}} \hat{R}_i \tag{11}$$

where D_{eff} is calculated based on the Chapman-Enskog binary diffusivities of CO and CO_2, bed porosity and tortuosity, assuming ideal gas behavior.

The domain of this problem is assumed to be based on a button cell configuration, and is taken as a cylinder with radius r_o, equal to the inner radius of the anode chamber, and height, h, equal to the depth of the particle bed, as shown in Fig. 1. The boundary condition at the right of the bed ($r = r_o$), is modeled as an open surface where any mass flux out of the system is due to convection. The anode surfaces (z = 0 and z = h) are modeled as a specified flux condition corresponding to a current density distribution i. The oxygen ion flux, j_o, into the system is related to i by $j_o = i/(2F)$, where F is Faraday's constant. A convective flux exists at the anode boundaries due to the oxidation of CO to CO_2, and these Stefan velocities, for the steam-carbon and air-carbon anode surfaces respectively, are given by

$$\vec{u}(r,0) = \left(\frac{1}{2F} \right) \left(\frac{\hat{M}_{CO_2} - \hat{M}_{CO}}{\rho} \right) \hat{z} \tag{12}$$

$$\vec{u}(r,h) = -\left(\frac{1}{2F} \right) \left(\frac{\hat{M}_{CO_2} - \hat{M}_{CO}}{\rho} \right) \hat{z} \tag{13}$$

The current density distribution i at each anode surface was found by calculating the current density distribution that produced a given voltage for the cell. These voltages, E_{steam} and E_{air} for the steam-carbon and air-carbon cells respectively, were inputs to the model and each is related to the various loss mechanisms in its respective cell by the relation

$$E = E_{OCV} - n_{electrolyte} - n_{anode} - n_{cathode}, \tag{14}$$

where E_{OCV} is the open circuit voltage of the cell at the reactant concentrations solved for at the electrode surfaces, $n_{electrolyte}$ is the voltage loss from ion conduction through the YSZ electrolyte, and n_{anode} and $n_{cathode}$ are the activation losses from the anode and cathode, respectively. E_{OCV} is directly calculated for each cell using the Nernst equation, where the concentrations of the gas species at the electrode surfaces are calculated directly from the model itself. This means that mass transport losses are included in this term and do not need to be added separately.

The cell voltage loss for each cell from oxygen ion conduction through the electrolyte, $n_{electrolyte}$, is calculated based on ohm's law

$$n_{electrolyte} = i\frac{t_e}{\sigma}. \tag{15}$$

Here, σ is the conductivity of YSZ at temperature T and is found from published values.

The activation overpotentials at the anode and cathode, n_{anode} and $n_{cathode}$, are calculated using a Butler-Volmer model of electrode kinetics. The current density i is related to the overpotential for an electrode through the relation

$$i = i_0\left\{e^{\alpha\frac{nF}{RT}\eta} - e^{(\alpha-1)\frac{nF}{RT}\eta}\right\}. \tag{16}$$

The exchange current density is assumed to follow an Arrhenius form in the temperature regime of interest, and values of A and E for the oxidation of CO and the reduction of steam on the Ni/YSZ system as well as the reduction of oxygen on the LSM/YSZ system, were calculated based on EIS data of the steam-carbon cell. The results are shown in Table II.

Table II: Arrhenius Parameters of Electrode Reactions

	Pre-Exponential (A) [mA/cm^2]	**Activation Energy (E_a)** [kJ/mol]	**Charge coefficient (α)**
CO Oxidation	4.31×10^{-1}	73 ± 7	0.48
H_2O Reduction	2.42×10^{3}	175 ± 17	0.47

Reliable published results for the activation energy of carbon monoxide oxidation on a Ni-YSZ anode are limited and scattered. One report on CO kinetics on Ni/YSZ bounds the overall activation enthalpy between 41 kJ/mol and 158.1 kJ/mol based upon the energies for some of the elementary reaction steps measured by the authors, although the rate limiting step was not determined [22]. Other studies have calculated

values ranging from 59.8 kJ/mol [23] to 136 kJ/mol [24] and even as high as 165 kJ/mol [25]. The values found in this study fall within this expected range. Studies on steam electrolysis in a solid oxide electrolysis cell place the value for steam reduction on Ni/YSZ at 192 kJ/mol in one study [26] and between 86.8 kJ/mol and 125 kJ/mol in another [27]. Regardless, the measured value in this study is within reason and is the largest of all the reactions studied, as expected. The values for the oxygen reduction on LSM are derived in a similar fashion on an air-carbon cell.

In the two cathode chambers, gas phase convection and diffusion velocity vectors are found by solving the Navier-Stokes equations along with the diffusion equation

$$\rho\frac{D\vec{v}}{Dt} = -\nabla p + \mu\nabla^2\vec{v}, \tag{17}$$

$$\frac{\partial\rho}{dt} + \rho\left(\nabla\cdot\vec{v}\right) = 0, \tag{18}$$

$$J_k = -D\nabla C_k. \tag{19}$$

For the steam-carbon cell, the binary diffusion coefficient for hydrogen and water is used. For the air-carbon cell, a binary mixture of oxygen and nitrogen is assumed. At the cathode surfaces, a Stefan flux exists due to the reduction of water to hydrogen and the reduction of oxygen, and these boundary conditions for the air-carbon and steam-carbon cell are respectively represented as

$$\vec{u}(r,h) = \left(\frac{1}{4F}\right)\left(\frac{-\hat{M}_{O_2}}{\rho}\right)\hat{z} \tag{20}$$

$$\vec{u}(r,0) = -\left(\frac{1}{2F}\right)\left(\frac{\hat{M}_{H_2} - \hat{M}_{H_2O}}{\rho}\right)\hat{z} \tag{21}$$

The electrical interactions between the air-carbon and steam-carbon cells in the SCAFC model was designed in such a way as to allow for voltage and current mismatches between the two cells by the integration of a parallel and series source or load into the circuit diagram, as shown in Figure 5. The parallel load and the series load both serve to either draw out electrical power or supply needed electrical power if there is a current or voltage difference between the two cells.

The model is implemented in Matlab, and uses COMSOL, a multiphysics finite element software package, to solve the coupled equations. The solution is arrived through a nonlinear iterative solver with linearized solutions found at each step using the PARDISO sparse solver. In order to gain insight into the workings of the numerical model, it is useful to consider a simplified solution process first. If we consider only the air-carbon side, the coupled nature of the solution becomes apparent: The cell voltage, $E_{OCV,air\text{-}carbon}$, is dependent upon the local concentrations of reactant and product species, as defined by the Nernst equation. These local gas concentrations, however, depend upon the flux of oxygen ions into and out of each chamber through the electrolyte, which is an analog to the current density i_{air} in the

air-carbon cell. This current density, however, depends on the original unknown: the open circuit voltage $E_{OCV,air\text{-}carbon}$.

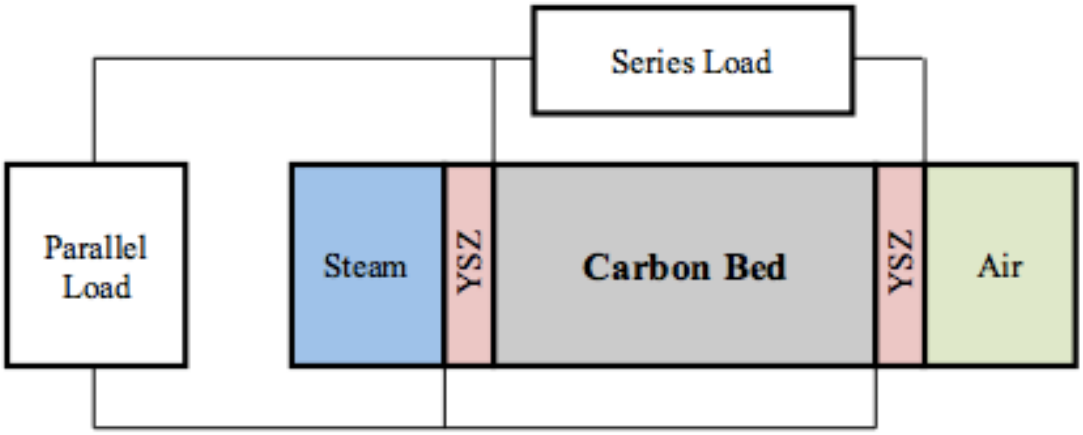

Figure 5: Electrical circuit diagram for the SCAFC model. The series and parallel loads and power sources allow for voltage and current mismatches between the two cells.

To overcome this coupling, a starting guess is given for the current density distribution i_{air} in the cell. This guess is based upon experimental I-V data and attempts to give the model a starting point near the eventual solution. This initial guess is used to solve for the gas phase concentrations throughout the system. These concentrations can then be utilized to calculate the cell open circuit voltage, $E_{OCV,air\text{-}carbon}$, and the cell current density distribution i_{air} at the cell voltage of interest $E_{air\text{-}carbon}$ is calculated from this value. This represents the start of the next iteration step. The new solution value for i_{air} is compared against the guess, and if these values match, the model has converged to a final valid solution. If the values differ, however, the new solution value of i_{air} is used as a new guess and the process is repeated until convergence is achieved.

The model utilizes a quasi-steady assumption, since the time scale for the gases in the bed to equilibrate into a steady condition is short compared to the time scale for char burnout. As a result, the dependence of the char bed physical parameters as a function of char conversion and therefore time, which directly impact the rate of char conversion in the bed, is not solved for by the model, but is instead fed into the model as an input by setting the char conversion parameter x_c, which is used to directly calculate the bed physical parameters at any point in time. The model therefore solves for the steady state conditions for a given set of parameters, which are set based upon the model input x_c.

Preliminary Sulfur Sorbent Predictions

Sulfur in coal poses a major bottleneck in advancing fuel cell technology for efficient coal conversion. Sulfur, a known poison for catalysts in general, rapidly deactivates the catalytic anode material and degrades the performance of fuel cells.

That is the reason why all fuel cell based programs such as SECA, which are founded on steam gasification of coal, employ separate and elaborate syngas cleanup processes. These gas cleanup steps require significant energy expenditure, resulting in lower conversion efficiencies than desired. Clearly, an all inclusive gas cleanup operation accomplished in the same process chamber that also houses the fuel cell stack offers great benefits in cost, simplicity, and thermal management, and is expected to result in higher overall system conversion efficiencies.

Ni, which is typically used as the catalyst in the cermet anode structure for solid oxide fuel cell, is deactivated by sulfur to form a volatile sulfide. There is also evidence of synergistic effects that the presence of sulfur in the form of H_2S magnifies and accelerates the cooperative deleterious effects of arsenic and phosphorus on cell performance through Ni anode degradation [17].

Thermodynamic equilibrium calculations were undertaken by Mitchell [18] to determine the composition of the synthesis gas and levels of trace species formed when Pittsburgh #8 coal, a widely used coal for power generation, is gasified in CO_2 at 1 atm under adiabatic autothermal conditions. On a percent-weight basis, Pittsburgh #8, a bituminous coal, contains 70.05% C, 4.55% H, 1.33% N, 1.33% S, 0.07% Cl, 6.81% O, 2,54% H_2O, and 13.32% ash. Shown in Fig. 6 are the calculated concentrations of the main species that contain sulfur, nitrogen and chlorine. At 1173 K, the H_2S, COS, and HCl concentrations are 2629, 397, and 144 ppmv, respectively. Ammonia and hydrogen cyanide concentrations are less than 1 ppmv.

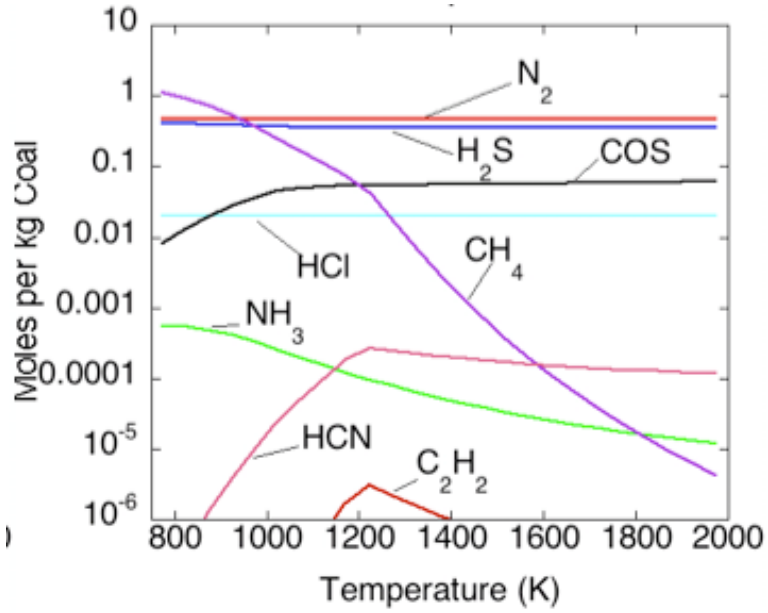

Figure 6. Calculated minor species concentration in syngas for autothermal dry gasification of Pittsburgh #8 coal at 1 atm.

The concentrations of the sulfur-containing species are too high for sustained fuel cell operation; the anode will be degraded due to sulfur poisoning. The concentrations of the species containing arsenic and phosphorus may be too high as

well. The concentrations of these species must be reduced before the technology is attractive at the commercial stage. Among the goals of this project is to identify sorbents capable of reducing the sulfur content of the syngas to less than 5 ppmv. Although arsenic and phosphorus trace levels present in coal may also cause anode degradation, our laboratory is not properly equipped to handle and test such toxic gases as arsine and phosphine. Hence, coal contaminants other than sulfur are not within the scope of this project. However, strategies employed to reduce sulfur levels in the syngas are likely to be effective in reducing the concentrations of other contaminants in the syngas as well.

Calcium-based sorbents such as limestone (nominally calcite, $CaCO_3$) and dolomite ($CaMg(CO_3)_2$) have been found to be effective in removing SO_2 from combustion gases at temperatures as high as 1000 ˚C. Sulfur is captured as both $CaSO_4$ and $MgSO_4$. More than 95% sulfur capture has been reported [19]. Fluidized bed combustion of coal with limestone or dolomite injection to capture SO_2 is a well-established, commercially available technology. Limestones and dolomites have also been found to be effective sorbents in capturing H_2S and COS from coal gasification gases. Sulfur is captured as both CaS and MgS. Indeed, preliminary thermodynamic calculations shown in Fig. 7 indicate that solid sorbents may have the potential to effectively reduce the sulfur content in the syngas to levels tolerated by the catalytic anode material.

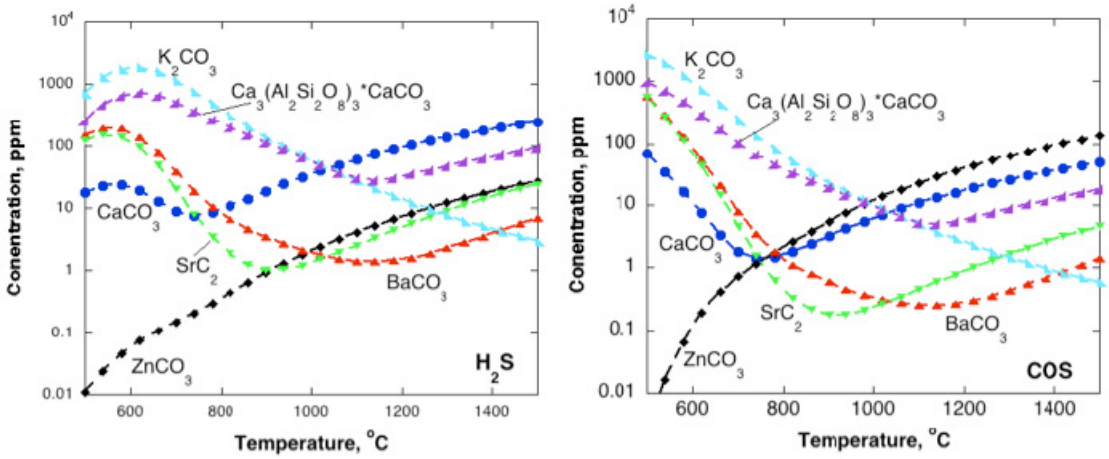

Figure 7: Equilibrium concentrations of H_2S and COS in syngas after addition of selected sorbents

Progress

The results from the preliminary modeling study are shown in Fig. 8. The calculated operational space is plotted to show the relationship between the three primary solution results of interest: the overall cell efficiency (shaded), the hydrogen production rate, and the electric power produced. Results with a negative electric power production value (P_{in} greater than 0) are not shown in the results.

The modeling results indicate that cell efficiency can vary widely over the operational space, with a maximum value of 82.6% and a minimum value of less than

1%. The results also show that the solution space folds back onto itself, and for any valid combination of electric power output and hydrogen production, there are two possible operating conditions, one with high efficiency and one with a low cell efficiency.

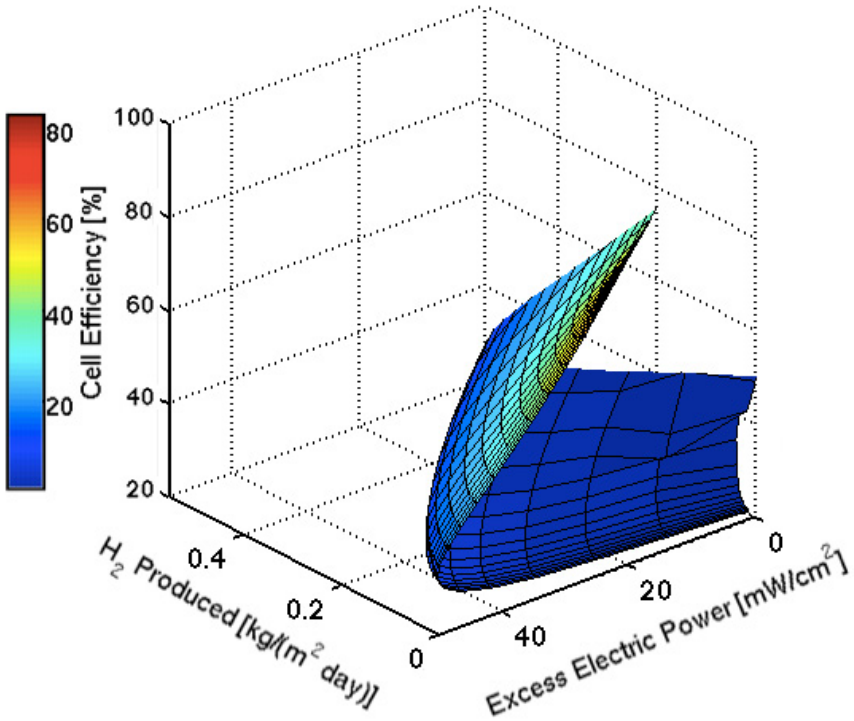

Figure 8: Operational space for the coupled fuel cell, as calculated by the integrated model. The overall cell efficiency is plotted as a function of hydrogen production and electric power production.

For a practical system, it is desirable to operate within regimes where the power output from both the parallel and series loads, $P_{parallel}$ and P_{series}, are both positive. Situations where the sum of these two are positive, but one of them negative, are undesirable because complex power electronics would be required to use the excess power from one block to supply the other. In addition, desirable operation will require no energy input, and therefore operational regimes where Q is non-positive (autothermal or heat rejection) are also ideal.

When these added conditions are placed upon the solution, a significant portion of the operational space shown in Fig. 8, representing the non-ideal operational regime, is removed. The requirement that P_{series} be positive results in most of the low efficiency portion of the operational space being discarded, and as a result a two dimensional contour view becomes possible to more easily visualize the results. The requirement of $P_{parallel}$ to remain positive removes a small parabola-shaped section at low electric power production rates, and the final requirement that the heat input Q be non-positive results in a slightly larger parabolic section being removed at low power

and hydrogen production rates. The resulting ideal operational space is shown as a contour plot in Fig. 9.

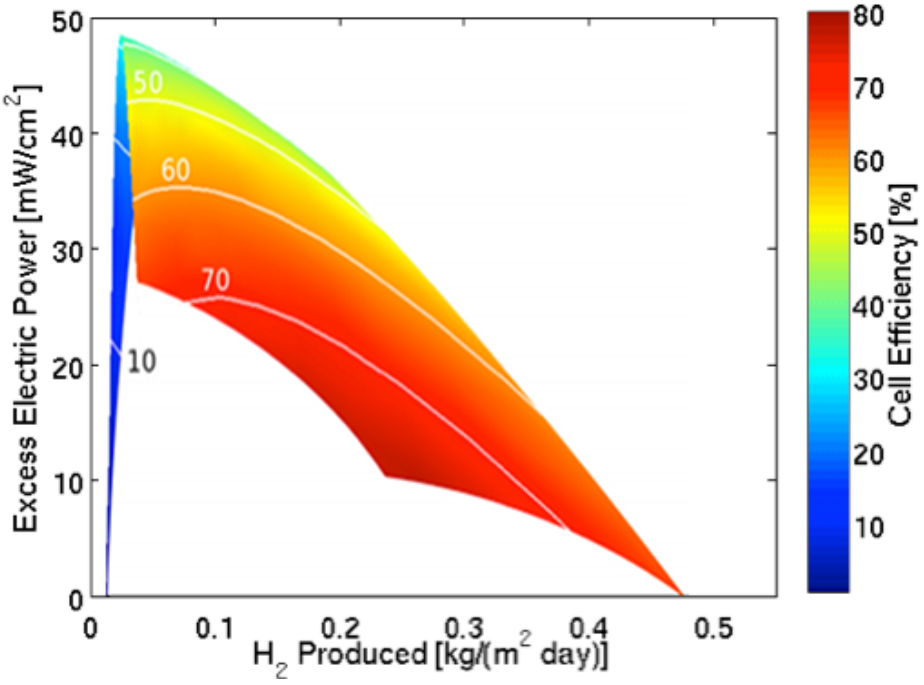

Figure 9: Ideal operation region for the coupled fuel cell, as calculated by the integrated model. Points that require any electric or heat input are not shown in the plot.

The ideal operational space results indicate that the SCAFC arrangement is able to efficiently produce hydrogen and electric power both spontaneously and without any external heat inputs. If efficiency is the primary motivating factor for cell operation, a maximum cell efficiency of over 76% can be realized by operating near the solution point which produces hydrogen at a rate of 0.223 kg/(m^2 day) and 14.2 mW/cm^2 of electric power. This operational point corresponds to voltages of 0.8 V on the air-carbon cell and -0.4 V on the steam-carbon cell. This point exists at the intersection of the autothermal contour and the zero $P_{parallel}$ contour in the solution space, meaning that no heat is required or rejected by the cell, and no power is removed or added through the parallel block in the circuit diagram. In effect, this means that although the cells are operating at different voltage levels, the total current passing through each cell is identical.

If hydrogen production is the primary goal, a maximum hydrogen production rate of approximately 0.447 kg/(m^2 day) with no electric output can be realized with an overall cell efficiency of 66.2%. This point exists at the location where both P_{series} and $P_{parallel}$ are equal to zero, meaning this point is where the air-carbon cell is fully overdriving the steam-carbon cell. This occurs when the current passing through both cells is equal and when the steam-carbon bias voltage is equal to the air-carbon cell voltage, near 0.6 V for this case. According to the model results, a steam-carbon fuel cell device could only produce 0.049 kg/(m^2 day) of hydrogen on its own

spontaneously, and would further require a heat input to keep the cell operational. By coupling the steam-carbon fuel cell and adding an air-carbon cell to both provide heat and more electric power, a nine-fold increase in hydrogen production rate density is realized with only a doubling in active cell area, and furthermore the heat input requirement is eliminated and overall cell efficiency is raised from 62.0% to 66.2%.

The results shown in this preliminary modeling study demonstrate that a steam-carbon-air fuel cell has the promise to deliver both hydrogen fuel and electric power from solid carbonaceous fuel sources without any external heat or power inputs. If hydrogen production alone is desired, the use of the coupled cell scheme allows for greater than nine-fold increase in hydrogen production rate density with only a twofold increase in active cell area, while both raising overall cell efficiency and eliminating the requirement for external heat addition. The model also predicts a high efficiency of over 76% for the couple fuel cell system producing both electric power and hydrogen at the same time.

Future Plans

During the next twelve months, we will execute our project plan proposed earlier. This will include materials screening and selection in several areas of the project, namely, for promising sulfur sorbents, for candidate materials for catalytic cathodes for steam and oxygen reduction reactions, and for potentially sulfur tolerant catalytic anodes. Naturally, this selection process will involve both experimental studies and thermodynamic predictions. Char reactivity studies are planned concurrently with materials selection tasks. Improving the system model beyond the preliminary stage to include heat transfer, geometric and design considerations will also be initiated later in the first year. A breakdown of the individual project tasks are summarized below in Table III.

Table III. Flow sheet of individual project tasks.

Task Name	Task Description	Year 1	Year 2	Year 3
Task 1	Coupled Steam-Carbon/Air-Carbon Fuel Cell Characterization			
Subtask 1.1	*Concept demonstration studies*			
Subtask 1.2	*Electrochemical cell performance studies*			
Task 2	Characterization and evaluation of prospective anodes			
Subtask 2.1	*CO electrochemical oxidation studies*			
Subtask 2.2	*Anode structure and microstructure characterization studies*			
Subtask 2.3	*Sulfur tolerant anode materials studies*			
Task 3	Steam Reduction Cathode Materials Studies			
Subtask 3.1	*Multifunctional cermet cathode studies*			
Subtask 3.2	*Cathode decoration and infiltration studies*			
Task 4	Identification of Suitable Sulfur Sorbents			
Subtask 4.1	*Dispersed sorbent synthesis*			
Subtask 4.2	*Sulfur uptake measurements*			
Subtask 4.3	*Sorbent regeneration studies*			
Task 5	Characterization of Coal/Biomass Char Conversion Rates			
Subtask 5.1	*Characterizing char reactivity to CO2*			
Subtask 5.2	*Characterizing char reactivity to O2*			
Subtask 5.3	*Characterizing char reactivity to H2O*			
Task 6	Integrated System Demonstration			
Task 7	System Modeling			
Task 8	Final Report Preparation			

As shown in Table III, parallel efforts are anticipated with fuel cell characterization and anode development studies (Tasks 1, 2 and 3) proceeding at nearly the same time as the sorbent, char conversion and system modeling studies

(Tasks 4, 5, and 7), activities in both groups starting at the beginning of the project. The framework for advanced modeling of the coupled fuel cell will begin in the second year of the project, with the model being updated as results from the other tasks become available.

On the administrative side, we have already identified and recruited two graduate students to work on various aspects of the research tasks. At the same time, we are actively searching for a postdoctoral fellow, but we have not identified a candidate yet. We will also identify and start acquiring soon the capital equipment planned for the successful conduct of this project.

Publications and Patents

1. Alexander, Brentan R., Mitchell, Reginald E. and Gür, Turgut M. *Viability of Coupled Steam-Carbon-Air Fuel Cell Concept for Spontaneous Co-production of Hydrogen and Electrical Power,* J. Electrochem. Soc. **159**, B810, 2012.

Note: This publication was not supported by GCEP but was conducted as a preliminary study in anticipation of a possible GCEP award.

References

1. Gür ,T. M. and Duskin A. *Steam-Carbon Cell for Hydrogen Production*, United States Patent Application: US 2008/0022593 A1, January 31, 2008.
2. Alexander, B. R., Mitchell, R. E., Gür, T. M. Viability of Coupled Steam-Carbon-Air Fuel Cell Concept for Spontaneous Co-Production of Hydrogen and Electric Power, *J. Electrochem. Soc. 159*:12, F810-F818, 2012.
3. Alexander, B. R., Mitchell, R. E. and Gür, T. M. *Steam-Carbon Fuel Cell Concept for Cogeneration of Hydrogen and Electrical Power,* J. Electrochem. Soc. **158**(5), B505, 2011.
4. Lee, A. C., Mitchell, R. E., Gür, T. M. *Feasibility of Hydrogen Production in a Steam-Carbon Electrochemical Cell,* Solid State Ionics **192**, 607, 2011.
5. Lee, A. C., Li, S., Mitchell, R. E., Gür, T. M. *Conversion of Solid Carbonaceous Fuels in a Fluidized Bed Fuel Cell,* Electrochemical and Solid-State Letters, **11** (2) B20-B23, 2008.
6. Doenitz, W., Hermeking, H., Kitzmann, I., Koch, A., Roettenbacher, R., Schaefer, W., Schmidberger, R, Schumacher, J., Vonzuelow, H. "High Temperature Water Vapor Electrolysis (HOT ELLY)," Final Report, Dornier-Werke G.m.b.H., 1980.
7. NETL. "Solid State Energy Conversion Alliance (SECA)". 22 Apr. 2013. <http://www.netl.doe.gov/technologies/coalpower/fuelcells/seca/>
8. Homel, M., Gür, T. M.. Virkar, A. V. Carbon Monoxide Fueled Solid Oxide Fuel Cell, J. Power Sources 195, 6367, 2010.
9. Gür, T. M., Homel, M., Virkar, A. V. "High Performance Solid Oxide Fuel Cell Operating on Dry Gasified Coal," J. Power Sources 195, 1085, 2010.
10. Li, S., Lee, A. C., Mitchell, R. E., Gür, T. M. "Direct Carbon Conversion in a Helium Fluidized Bed Fuel Cell," Solid State Ionics 179, 1549-1552, 2008.
11. Gür, T. M. *J. Electrochem. Soc*. **157**(5), B571, 2010.
12. Horita, T., Sakai, N., Kawada, T., Yokokawa, H., and Dokiya, M. *J. Electrochem. Soc.* **142**(8), 2621, 1995.
13. Nakagawa, N. and Ishida, M. *Ind. Eng. Chem. Res.* 27, 1181, 1988.
14. Nürnberger, S., Bussar, R., Desclaux, P., Franke, B., Rzepka, M., and Stimming, U. *Energy Eneviron. Sci.* 3, 150, 2010.
15. Wu, Y., Su, C., Zhang, C., Ran, R., and Shao, Z. Z. *Electrochemistry Comm.* 11, 1265, 2009.
16. Lee, A. C., Mitchell, R. E., Gür, T. M. *AIChE Journal* **55**(4), 983, 2009.
17. Ma, L. *Combustion and Gasification of Chars in Oxygen and Carbon Dioxide at Elevated Pressure [Dissertation]*. Stanford, CA: Mechanical Engineering Dept., Stanford University, 2006.
18. Teller, E., Brunauer, S., Emmett, P.H. *J. Am. Chem. Soc.* **60**: 309-319, 1938.

19. Rounsley, R. R. *J. AIChE* **7**(2), 308-311, 1961.
20. Bhatia S. K., Perlmutter D. D. *AIChE J.* **26**:379–386, 1980.
21. Bird, R. B., Stewart, W. E., and Lightfoot, E. N. Transport Phenomena. Wiley, New York, 1960.
22. Yurkiv, V., Starukhin, D., Volpp, H.-R., Bessler, W. G. *Journal of The Electrochemical Society*, **158**:1, B5-B10, 2011.
23. Sukeshini, A. M., Habibzadeh, B., Becker, B. P., Stoltz, C. A., Eichhorn, B. W., and Jackson, G. S. *Journal of The Electrochemical Society,* **153**:4, A705-A715, 2006.
24. Utz, A., Leonide, *., Weber, A., Ivers-Tiffée, E. *Journal of Power Sources* 196, 7217–7224, 2011.
25. Shi, Y., Li, C., Cai, N. *Journal of Power Sources* 196, 5526–5537, 2011.
26. Marina, O. A., Pederson, L. R., Williams, M. C., Coffey, G. W., Meinhardt, K. D., Nguyen, C. D., Thomsena, E. C. *Journal of The Electrochemical Society,* **154** :5, B452-B459, 2007.
27. Olmer, L. J., Viguie, J. C., Schouler, E. J. L. *Solid State Ionics*, **7**:23, 1982.

Contacts:

Reginald E. Mitchell: remitche@stanford.edu

Turgut M. Gür: turgut@stanford.edu

David U. Johnson: daviduj@stanford.edu

Kevin Steinberger: ksteinbe@stanford.edu